Histol Histopathol (2015) 30: 489-501
DOI: 10.14670/HH-30.489

http://www.hh.um.es

Histology and Histopathology
Cellular and Molecular Biology

Differential effects of intestinal ischemia and reperfusion in rat enteric neurons and glial cells expressing P2X2 receptors

Aline Rosa Marosti[1], Marcos Vinícius da Silva[1], Kelly Palombit[1], Cristina Eusébio Mendes[1], Wothan Tavares-de-Lima[2] and Patricia Castelucci[1]

[1]Department of Anatomy and [2]Department of Pharmacology/Biomedical Science Institute, University of São Paulo, São Paulo, Brazil

Summary. *Background*. Intestinal ischemia followed by reperfusion (I/R) may occur following intestinal obstruction. In rats, I/R in the small intestine leads to structural changes accompanied by neuronal death.

Aim. The objective was to analyze the impact of I/R injury on different neuronal populations in the myenteric plexus of the rat ileum after different periods of reperfusion.

Methods. The superior mesentery artery was occluded for 45 minutes, and animals were euthanized after 24 hours and 1 week of reperfusion. Immunohistochemical analyses were performed with antibodies against the P2X2 receptor in combination with antibodies against nitric oxide synthase (NOS), choline acetyltransferase (ChAT), calbindin, calretinin, the pan-neuronal marker anti-HuC/D, or S100β (glial marker).

Results. Dual immunolabeling demonstrated that approximately 100% of NOS-, ChAT-, calbindin-, and calretinin-immunoreactive neurons in all groups expressed the P2X2 receptor. Following I/R, the neuronal density decreased in the P2X2 receptor-, ChAT-, calretinin-, and HuC/D-immunoreactive neurons at 24 hours and 1 week following injury compared to the densities in the control and sham groups. The calbindin-immunoreactive neuron density was not reduced in any of the groups. The density of enteric glial cells increased by 40% in the I/R group compared to the density in the sham groups. We also observed increases of 12%, 16%, and 23% in the neuronal cell body profile areas of the NOS-, ChAT-, and calbindin-immunoreactive neurons, respectively, at 1 week following I/R. However, the average size of the calretinin-immunoreactive neurons was reduced by 12% in the I/R group at 24 hours.

Conclusions This work demonstrates that I/R is associated with a significant loss of different classes of neurons in the myenteric plexus accompanied by morphological changes and an increased density of enteric glial cells; all of these effects may underlie conditions related to intestinal motility disorder.

Key words: Chemical coding, Myenteric neurons, Ischemia and reperfusion, P2X2 receptor, Enteric glial cell.

Offprint requests to: Dr. Patricia Castelucci, PhD, Assistant Professor, Department of Anatomy, Institute of Biomedical Sciences, University of São Paulo, Av. Prof. Dr. Lineu Prestes, 2415, CEP 05508-900, São Paulo, Brazil. e-mail: pcastel@usp.br

Introduction

Acute mesenteric ischemia results from a total or partial interruption of blood flow to the intestine that causes depletion in the supply of oxygen and nutrients to a particular area; these effects can cause irreversible damage within a few hours. Acute mesenteric ischemia is caused by embolism, thrombosis, or spasm of mesenteric vessels (Oldenburg et al., 2004). Many physiological and pathological processes of the gastrointestinal tract rely on the integrity of the enteric nervous system, which is essential for a normal life. The enteric nervous system of the ileum is composed of the myenteric and submucosal plexuses, which control

motility, transport of fluids from the mucosa, and local blood flow (Furness, 2006). Structural support and maintenance of neurons is provided by enteric glial cells (Gabella, 1972). Studies have demonstrated a decrease in the total population of enteric neurons in rats submitted to ischemia and reperfusion (I/R), which may be indicative of neuronal death (Piao et al., 1999; Lindeström and Ekblad, 2004). Studies of the consequences and mechanisms of I/R injury in the intestine indicate that certain neuronal subtypes may be more affected. Ischemia can lead to a significant increase in the number of vasoactive intestinal peptide (VIP)-immunoreactive and nitric oxide synthase (NOS) cell bodies in the myenteric plexus in the rat small intestine (Calcina et al., 2005); in guinea pigs, ischemia can lead to changes in the morphology of neurons immunoreactive for nitric oxide synthase (NOS) and calbindin (Rivera et al., 2009).

Studies have shown that many gastrointestinal motor responses may also be mediated by adenosine triphosphate (ATP), which binds to P2X receptors in the myenteric plexus (Abbrachio et al., 2009). Immunohistochemical studies have identified the presence of the P2X2 (Vulchanova et al., 1996; Castelucci et al., 2002a,b; Xiang and Burnstock, 2005), P2X3 (Poole et al., 2002; Van Nassauw et al., 2002), P2X6 (Yu et al., 2010), and P2X7 (Hu et al., 2001) receptors in the enteric nervous system. In addition, studies have observed the presence of P2X7 (Vanderwinden et al., 2003) and P2Y4 (Van Nassauw et al., 2006) receptors in the glial cell of the rat gastrointestinal tract.

Processes such as I/R have also been associated with a significant loss of different subpopulations of neurons in the myenteric plexus that express P2X2 and P2X7 receptors and are accompanied by morphological changes, which may be related to intestinal motility disorders (Paulino et al., 2011; Palombit et al., 2013). Paulino et al. (2011) analyzed the effects of ischemia in the superior mesentery artery following 4 hours of reperfusion; however, the P2X2 receptor in the enteric neurons' chemical coding and the enteric glial cells in the ischemia in the same artery after prolonged reperfusion have not been analyzed.

In this present work, we analyzed the effects of ischemia in the superior mesentery artery followed by 24 hours and 1 week of reperfusion on NOS-, calretinin-, calbindin-, ChAT-, and enteric glial-immunoreactive cells co-expressing the P2X2 receptor in the rat ileal myenteric plexus.

Materials and methods

This study was conducted according to current regulations regarding animal experiments at the Biomedical Science Institute of the University of São Paulo. Young male Wistar rats (200–240 g body weight) were maintained under standard conditions at 21°C with a 12-h light-dark cycle, and all groups were supplied with water *ad libitum*.

Induction of ischemia

Rats were anesthetized with a mixture of xylazine (20 mg/kg) and ketamine hydrochloride (100 mg/kg) via intramuscular injection. The small intestine was exposed via a midline incision, and the superior mesenteric artery was located and occluded for 45 minutes with an atraumatic microsurgical vascular clamp (Vascu-statt). Intestinal reperfusion was reestablished by clip release. In the sham-operated groups, rats were subjected to identical manipulations without the arterial occlusion. The control animals were not submitted to the manipulations. The viscera were repositioned in the abdominal cavity, and the midline incision was closed with two layers of nylon monofilament sutures. At 24 hours and one week after reperfusion, animals were weighed and then sacrificed in a CO_2 chamber. The anterior abdominal wall was opened, and the small intestine was removed and washed in phosphate buffered saline (PBS; 0.15 M NaCl in 0.01 M sodium phosphate buffer, pH 7.2). Five rat ilea were analyzed from each group, i.e., the ischemic group (I/R-i), the sham group (sham), and the control group.

Fresh segments of ileum from each animal were dissected and placed in PBS containing nicardipine (10^{-6} M; Sigma, USA) to inhibit tissue contraction. The ileal segments were opened along the mesenteric border and cleaned of their contents with PBS. They were then pinned tautly open, with the mucosa side down, onto a balsa wood board and fixed overnight at 4°C in 4% paraformaldehyde in 0.2 M sodium phosphate buffer (pH 7.3). The next day, the tissue was cleared of fixative using three 10-minute washes in 100% dimethylsulfoxide (DMSO) followed by three 10-minute washes in PBS. All tissues were stored at 4°C in PBS containing sodium azide (0.1%). The fixed tissue was subdissected to remove the mucosa, submucosa, and circular layers, yielding whole mounts of longitudinal muscle-myenteric plexus. Whole-mount preparations of the myenteric plexus of the ileum were preincubated in 10% normal horse serum in PBS containing 1.5% Triton X-100 for 45 minutes at room temperature to reduce non-specific binding and to permeabilize the tissue (Table 1). To detect P2X2 receptor immunoreactivity, we used a rabbit antiserum raised against amino acid sequence 457-472 of the rat P2X2 receptor with a single Cys extension at the N-terminus (AB5244 from Chemicon, Temecula, CA, USA). Whole-mount preparations were incubated with the antibody for 48 hours at 4°C at a dilution of 1:120. Dual labeling was achieved using the combinations of antisera listed in Table 1. After incubation in primary antisera, tissues were washed three times for 10 minutes in PBS and incubated with various secondary antibodies (Table 2). PBS washes were repeated, and the tissue was mounted in glycerol buffered with 0.5 M sodium carbonate (pH 8.6).

Preparations were examined using a Nikon 80i fluorescence microscope. Images were captured using a digital camera and the NIS Nikon software package. In addition, preparations were analyzed using confocal

microscopy on a Zeiss confocal scanning laser system installed on a Zeiss Axioplan 2 microscope. Images were collected at 512 X 512 pixels, and the thickness of each optical section was 0.5 μm. Z-stacks of immunoreactive cells were captured as a series of optical sections with a center spacing of 0.2 μm. Confocal images were collected using LSM 5 Image Zeiss processing software and further processed using Corel Photo Paint and Corel Draw software.

Quantitative analyses

Antigen colocalization was assessed by examining fluorescently labeled preparations. Neurons were identified by immunofluorescence; the filter was then switched, and labeling for the second antigen was evaluated. The proportion of neurons labeled for antigen pairs was determined. The cohort size was 100 neurons per animal, and data were collected from preparations obtained from five animals. The percentage of dual-immunoreactive neurons was calculated and expressed as the mean ± standard error of the mean (SEM; n= number of preparations). The number of cells immunoreactive for the P2X2 receptor, NOS, calbindin, calretinin, ChAT, anti-HuC/D, and S100β, as well as neuronal morphological profiles, were measured by examining the whole-mount preparations at 100X magnification. Immunoreactive neuronal cell bodies in the myenteric ganglia were counted in each visual microscopic field (0.04909 mm^2). For quantification of the two whole-mount preparations (1.0 cm^2 each), counts were performed in 40 microscopic fields chosen at random for each antigen in each animal. The cell perikaryal profile areas (μm^2) of 100 randomly selected neurons from each animal were obtained using a semiautomatic morphometry device and measured using the Image Pro Plus software package. Data were compared by analysis of variance (ANOVA) and Tukey's test for multiple comparisons, as appropriate. $P<0.05$ was considered statistically significant.

Histology

The ileum region was removed and placed in PBS (0.15 M NaCl in 0.01 M sodium phosphate buffer, pH 7.2) containing nicardipine (10-6 M; Sigma, Sydney, Australia). The ileum was cleaned of its contents, opened along the mesenteric attachment, pinned (mucosa down) to balsa wood sheets without being stretched, and fixed in 10% formaldehyde in 0.1 M sodium phosphate buffer (pH 7.2) at 4°C. Each sample was placed in a histology cassette, dehydrated using a graded series of ethanol and histolene, and embedded in paraffin. Sections were cut transversely at a thickness of 5 μm and processed for standard hematoxylin and eosin (H&E) staining. Following the staining step, the tissue was mounted using a permanent mounting medium. Preparations were examined using a Nikon 80i microscope, and images were captured using a digital camera and the NIS Nikon software package.

Results

Qualitative analysis

P2X2 receptor immunoreactivity was observed in the myenteric plexus, as well as in the smooth muscle, in the control, sham and intestinal I/R groups. Specifically, immunofluorescence was apparent in the cytoplasm and surface membranes of most ileal nerve cells (Fig. 1). Dual-labeling studies were conducted to identify P2X2 receptor-immunoreactive cells that were also immunoreactive for NOS, ChAT, calbindin, calretinin, anti-HuC/D, or S100β (Figs. 1, 2). In the control, sham, and I/R animals, NOS-immunoreactive neurons exhibited a Dogiel Type I morphology, whereas calretinin-immunoreactive neurons exhibited a Dogiel Type II morphology. Calbindin-immunoreactive neurons presented Dogiel Type I and II morphologies (Fig. 1). Colocalization between NOS and HuC/D as well as colocalization between ChAT and HuC/D were observed (Fig. 2). Dual-labeling of the P2X2 receptor with S100β confirmed that enteric glial cells expressed the receptor in the analyzed groups (Fig. 2).

The histological observations showed that the appearance of villi, circular and longitudinal muscle, and enteric neurons in the sham 24 hour and sham 1 week groups was preserved (Fig. 3A,D,G). Following 24 hours of ischemia, the top of the villi were restored; however, there were some clear spaces in the ganglion. After 1 week of reperfusion, the villi were completely restored, no damage was visualized in the circular and longitudinal muscle, and the clear spaces were

Table 1. Characteristics of the primary antibodies used in this study.

Antigen	Host	Dilution	Code and reference
P2X2 Receptor	Rabbit	1:120	Chemicon
NOS	Sheep	1:2000	EMSO
Calretinin	Goat	1:100	Swant
Calbindin	Mouse	1:500	Swant
ChAT	Goat	1:50	Chemicon
Anti-HuC/D	Mouse	1:100	Molecular Probes
S100β	Mouse	1:300	Chemicon

Table 2. Secondary antibodies used in this study.

Antibody	Dilution	Source
Donkey anti-rabbit IgG 488	1:500	Molecular Probes
Donkey anti-sheep IgG 594	1:100	Molecular Probes
Donkey anti-mouse IgG 594	1:200	Molecular Probes
Donkey anti-sheep IgG 488	1:500	Molecular Probes

commonly larger and more prominent. The majority of neuron cells in the I/R 1 week group were affected by the treatment, as evidenced by a foamy cytoplasm, irregular cell shapes, and pyknotic and displaced nuclei (Fig. 3C,F,I).

Quantitative analysis

P2X2 Colocalization

In the myenteric plexus, the majority of NOS-

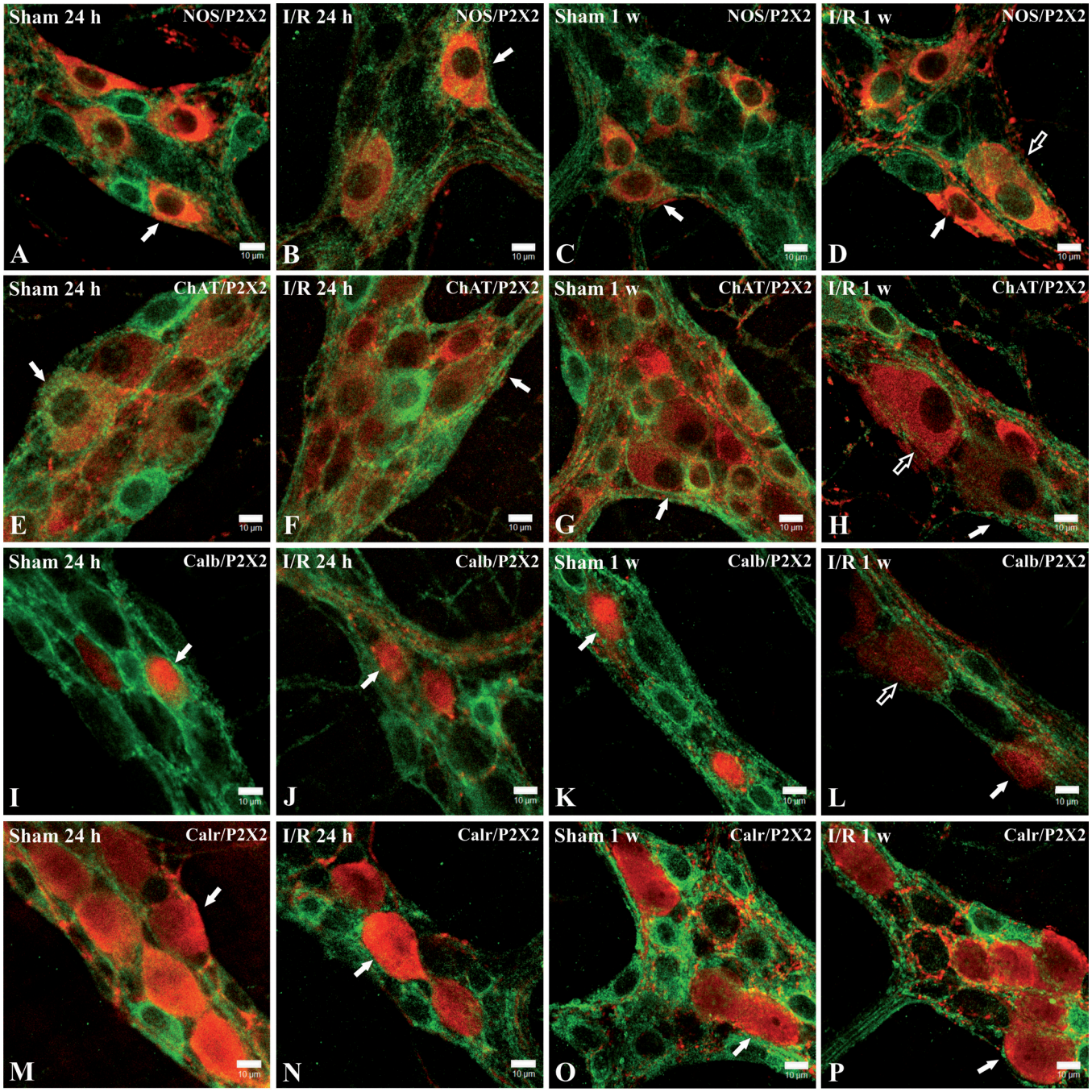

Fig. 1. Colocalization of P2X2 receptor (P2X2) immunoreactivity with nitric oxide synthase (NOS), choline acetyltransferase (ChAT), calbindin (Calb), and calretinin immunoreactivity in neurons of the rat ileum myenteric plexus in the sham and I/R (24 hour and 1week) groups. NOS immunoreactivity (red; **A-D**) colocalized with P2X2 immunoreactivity (green; **A**, **B**, **C**, and **D**). ChAT immunoreactivity (red; **E-H** colocalized with P2X2 immunoreactivity (green; **E-H**. Calb immunoreactivity (red; **I-L**) colocalized with P2X2 immunoreactivity (green; **I-L**). Calretinin immunoreactivity (red; **M-Q**) colocalized with P2X2 immunoreactivity (green; **M-Q**). Single arrows indicate dual-labeled neurons. Scale bars: 10 μm.

immunoreactive neurons were also immunoreactive for the P2X2 receptor (the control, sham 24 hour, I/R 24 hour, sham 1 week, and I/R 1 week groups were 99.7%±0.6%, 100%, 99.9±0.2%, 100%, and 100% colocalized, respectively). The majority of ChAT-immunoreactive neurons were also positive for the P2X2 receptor (the control, sham 24 hour, I/R 24 hour, sham 1 week, and I/R 1 week groups were 97.5%±1.2%,

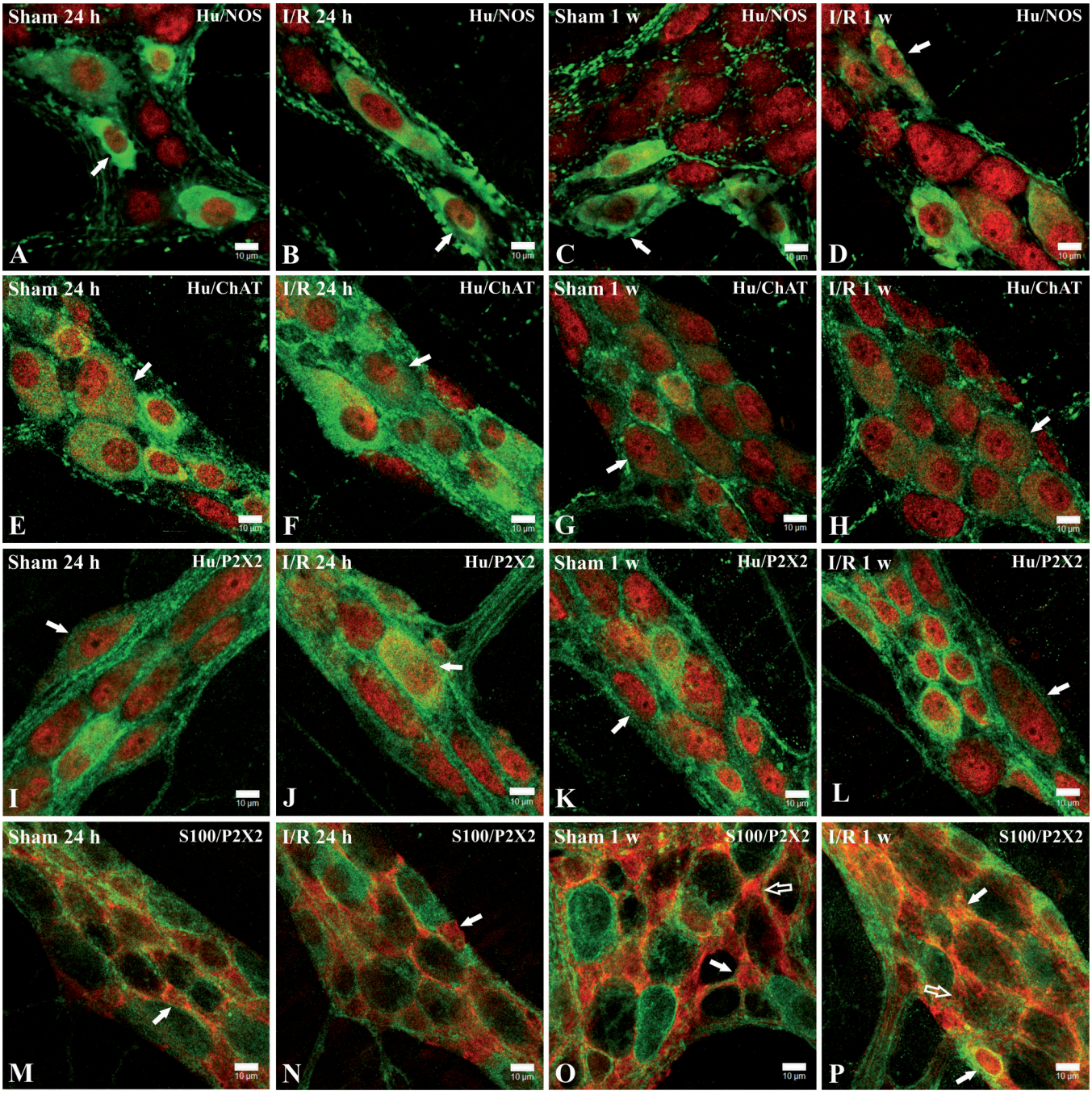

Fig. 2. Colocalization of HuC/D (Hu)-immunoreactivity with NOS, ChAT, and P2X2 receptor (P2X2) immunoreactivity in neurons of the rat myenteric plexus in the sham and I/R (24 hour and 1 week) groups. Hu immunoreactivity (red) colocalized with NOS immunoreactivity (green; **A-D**). Hu immunoreactivity (red) colocalized with ChAT immunoreactivity (green; **E-H**). Hu immunoreactivity (red) colocalized with P2X2 immunoreactivity (green; **I-L**). S100β immunoreactivity (red) colocalized with P2X2 immunoreactivity (green; **M-P**). Arrows indicate dual-labeled neurons and empty arrows indicate dual-labeled glial cells. Scale bars: 10 μm.

97.7±1.3%, 94.4±2.7%, 98.4±0.6%, 98.2±0.5% colocalized, respectively). The majority of calbindin-immunoreactive neurons were also immunoreactive for the P2X2 receptor (the control group was 93.8%±1%, the sham 24 hour group was 94.7±1.3%, the I/R 24 hour group was 93.8±0.9%, the sham 1 week group was 94.1±0.6%, and I/R 1 week group was 95.2±0.4% colocalized). One hundred percent of calretinin-immunoreactive neurons were immunoreactive for the P2X2 receptor in the control, sham 24 hour, I/R 24 hour, sham 1 week, and I/R 1 week groups.

The majority of S100β-immunoreactive enteric glial cells were immunoreactive for the P2X2 receptor in the control, sham 24 hour, I/R 24 hour, sham 1 week, and I/R 1 week groups (87.8±1.6%, 90.1±0.5%, 92.2±1.6%, 87.5±1% and 87.9±2.1 colocalized, respectively).

HuC/D colocalization

We found that 20.2±2.8%, 23.9±2.3%, 24.9±1.4%, 23.3±1.1%, and 28.4±1.2 of HuC/D-immunoreactive neurons were also positive for NOS in the control, sham 24 hour, I/R 24 hour, sham 1 week, and I/R 1 week groups (P>0.05), respectively. In addition, 100% of NOS-immunoreactive neurons were also immunoreactive for HuC/D in all groups. We found that 75.3±2.4%, 72.1±2.9%, 75±3%, 72.2%±1.6%, and 77.4±1.5% of HuC/D-immunoreactive neurons were

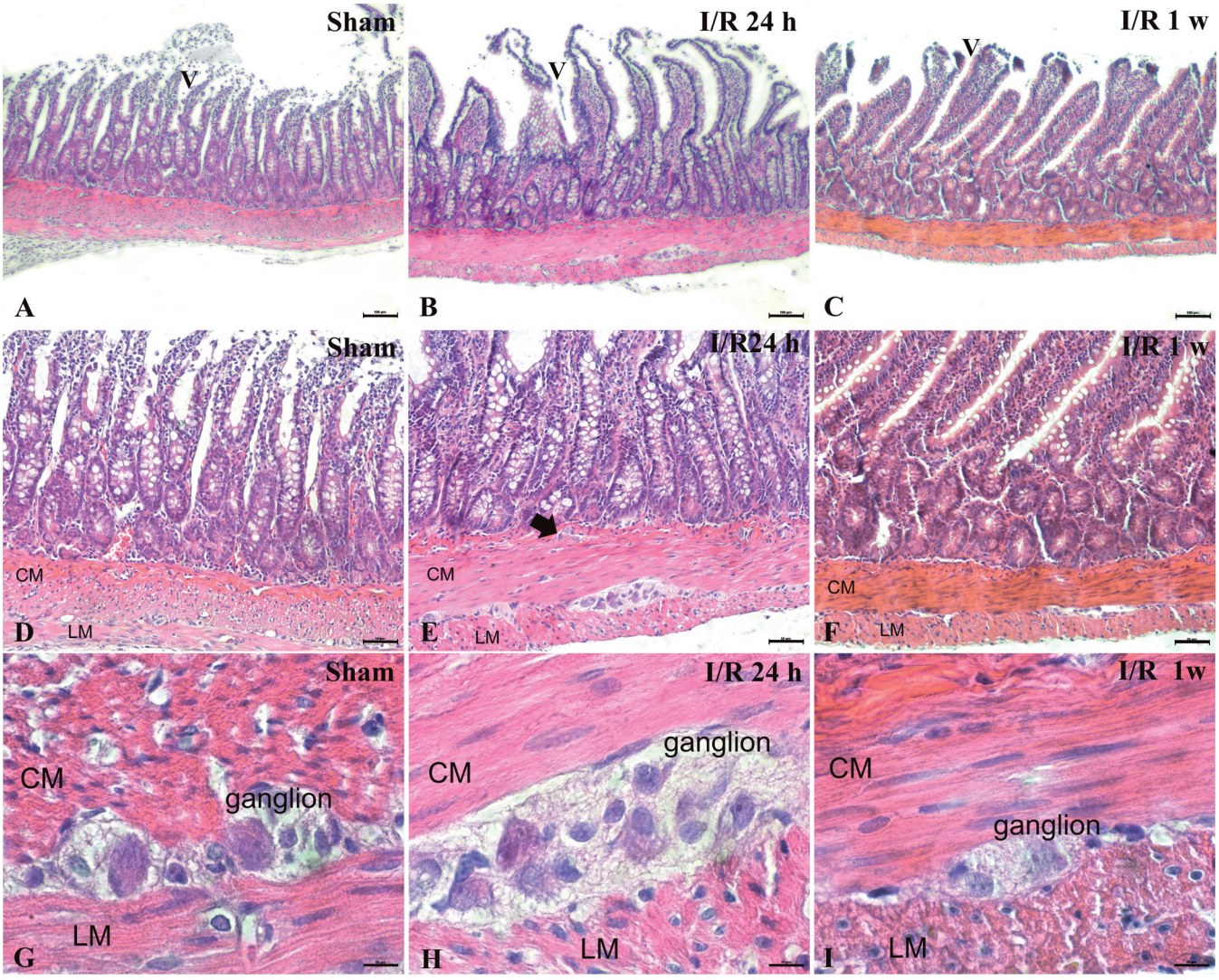

Fig. 3. Histological aspects following ischemia and reperfusion in the ileum. In sham-operated animals, the villi (V) **(A),** circular and longitudinal muscle **(D)**, and enteric ganglion **(G)** had normal structures after 24 hours. After 24 hours of reperfusion, the stumps of villi were commonly sealed **(B)**, the circular (CM) and longitudinal muscle (LM) **(E)** had a normal appearance, and there were more spaces within the ganglion (**H**) compared to the sham group. Following 1 week of reperfusion, the appearance of the villi, CM, and LM was similar to the sham group; inside the ganglion, there were also spaces in the I/R 24 hour group. Scale bars: **A-C**, 100 μm; **D-F**, 50 μm; **G-I**, 10 μm.

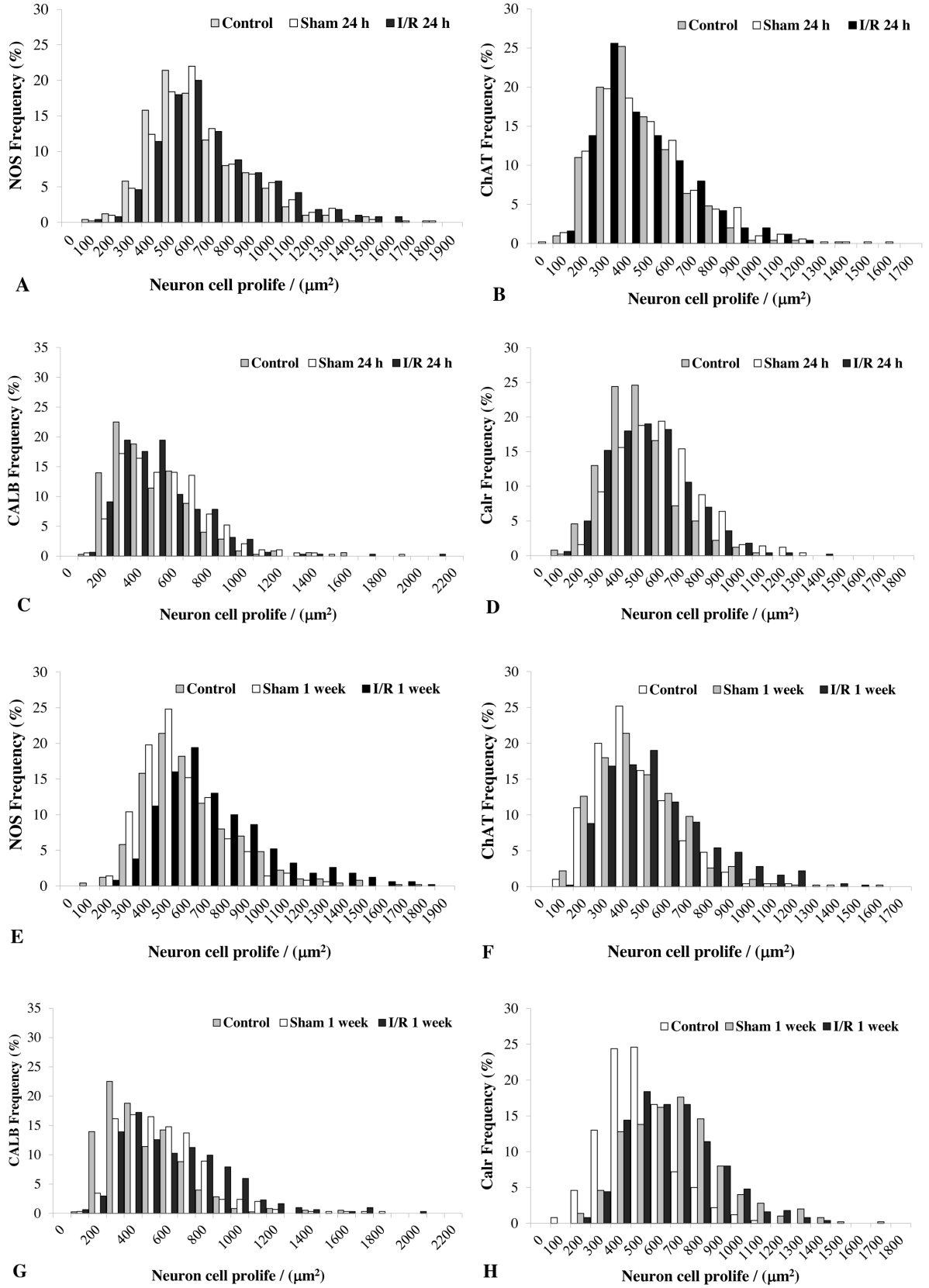

Fig. 4. Histogram showing the distribution of the areas (μm^2) of neurons immunoreactive for NOS (**A** - control, sham 24 hour and I/R 24 hour; **E** - control, sham 1 week, and I/R 1 week), ChAT (**B** - control, sham 24 hour and I/R 24 hour; **F** - control, sham 1 week and I/R 1 week), calbindin (**C** - control, sham 24 hour and I/R 24 hour; **G** - control, sham 1 week and I/R 1 week) and calretinin (Calr, **D** - control, sham 24 hour and I/R 24 hour; **H** - control, sham 1 week and I/R 1 week) in the neurons of the rat ileal myenteric plexus from the control, sham, and I/R (24 hour and 1 week) groups.

Table 3. Density of cells (neurons/cm^2) expressing the P2X2 receptor; neurons expressing NOS, ChAT, calbindin, calretinin, and HuC/D; and glial cells expressing S100β in the rat ileum myenteric plexus from the control, sham, and I/R (24 hour and 1 week) groups.

Immunoreactivity	Control	Sham 24 h	I/R 24 h	Sham 1 week	I/R 1 week
P2X2	14500±969	13026±172	11276±836$^{\beta}$	20329±982$^{\beta}$	18592±602$^{\pi}$
NOS	3382±445	4105±637	4237±703	3789±295	3326±253
ChAT	12395±466	11789±975	10421±194$^{\beta}$	13066±649	9184±640$^{\pi}$
Calbindin	1224±107	1,079±68	1026±45	1053±72	1118±72
Calretinin	4908±224	4566±220	4342±416	5434±323	5710±258$^{\gamma}$
Hu	19671±835	18210±951	16776±957$^{\beta}$	20079±799	16671±1097$^{\pi}$
S100β	20066±803	18684±556	26316±356$^{\beta}$	26158±904$^{\#\beta}$	34802±972$^{\pi\gamma}$

Data are expressed as the mean ± standard deviation ($^{\#}$compared to Control; $^{\beta}$compared to Sham 24 h; $^{\pi}$compared to Sham 1 week; $^{\gamma}$difference between 1 week and 24 h; $^{\#, \beta, \pi}$ p<0.05 or p<0.01 and $^{\gamma}$ p<0.01).

Table 4. Cell body profile (area in μm^2) of neurons immunoreactive for NOS, ChAT, calbindin, and calretinin in the rat ileum myenteric plexus of the control, sham, and I/R (24 hour and 1 week) groups.

Immuno-reactivity	Control	Sham 24 h	I/R 24 h	Sham 1 week	I/R 1 week
NOS	677±31	703±25	734±28	611±20$^{\beta}$	762±25$^{\pi}$
ChAT	502±7	533±32	503±23	509±17	584±19$^{\pi\gamma}$
Calbindin	522±17	600±11	557±40	614±38	683±29$^{\gamma}$
Calretinin	547±28	642±21	575±36$^{\pi}$	723±43$^{\#}$	698±14$^{\gamma}$

Data are expressed as the mean±standard deviation ($^{\#}$compared to Control; $^{\beta}$compared to Sham 24 h; $^{\pi}$compared to Sham 1 week; $^{\gamma}$difference between 1 week and 24 h; $^{\#, \beta, \pi}$ p<0.05 or p<0.01 and $^{\gamma}$ p<0.0

ChAT-immunoreactive in the control, sham 24 hour, I/R 24 hour, sham 1 week, and I/R 1 week animals, respectively. Inversely, 100% of ChAT-immunoreactive neurons also expressed HuC/D in all groups. In addition, we found that 99.4±0.4%, 99.6±0.4%, 99.4±0.4%, 99.2%±0.2%, and 99.4±0.4% of HuC/D-immunoreactive neurons were P2X2-immunoreactive in the control, sham 24 hour, I/R 24 hour, sham 1 week, and I/R 1 week animals, respectively. We found that 87.9±1.2%, 87.1±1%, 84.6±1.9%, 77.5%±0.7%, and 70.6±1.1% of P2X2-immunoreactive cells were HuC/D-immunoreactive in the control, sham 24 hour, I/R 24 hour, sham 1 week, and I/R 1 week animals, respectively. In addition, we found that 12.1±1.2% (control), 12.9±1.2% (sham 24 hour), 15.4±0.4% (I/R 24 hour), 22.5%±0.7% (sham 1 week), and 29.4±0.4% (I/R 1 week) of P2X2-immunoreactive cells were not neurons.

Neuronal density

The density of neurons immunoreactive for the P2X2 receptor increased by 40% and 56% in the sham 1 week group relative to the densities in the control and sham 24 hour groups, respectively. The density of P2X2 receptor-immunoreactive neurons decreased by 13% and 8.5% in the I/R 24 hour and I/R 1 week groups, respectively, compared to densities in the sham groups (P<0.05). The density of P2X2 receptor-immunoreactive neurons increased by 65% in the I/R 1 week group compared to that of the I/R 24 hour group (P<0.05) (Table 3). In addition, there were changes in the density of NOS-immunoreactive neurons in I/R 1 week group compared to that of the sham 1 week group (P<0.05) (Table 3). The density of ChAT-immunoreactive neurons did not differ between the control and sham groups. The density of ChAT-immunoreactive neurons in the I/R group was reduced by 12% and 30% at 24 hours and 1 week, respectively, compared to the density in the sham group (P<0.01; Table 3). The density of calretinin-immunoreactive neurons did not differ between the control and sham groups or between the I/R 24 hour and sham groups. The density of calbindin-immunoreactive neurons did not differ between groups (P>0.05; Table 3). The density of calretinin-immunoreactive neurons increased by 31% in the I/R 1 week group compared to that in the sham 24 hour group (P<0.05; Table 3). Moreover, the density of HuC/D-immunoreactive neurons did not differ between the control and sham groups. The density of HuC/D-immunoreactive neurons decreased by 8% and 17% (P<0.05) in the I/R group at 24 hours and 1 week, respectively, compared to the sham group (Table 3).

The density of S100β-immunoreactive enteric glial cells increased by 30% and 40% in the sham 1 week group compared to that in the control and sham 24 hour groups, respectively. The density of S100β-immunoreactive enteric glial cells increased by 41% and 33% in the I/R 24 hour and I/R 1 week groups, respectively, compared to the sham groups (P<0.05; Table 3). The density of S100β-immunoreactive enteric glial cells increased by 32% in the I/R 1 week group compared to the I/R 24 hour group (P<0.05; Table 3).

Neuronal profile area

Due to the colocalization of P2X2 receptor immunoreactivity with NOS-, ChAT-, calretinin-, and calbindin-immunoreactive neurons, the analysis of the average size or profile area of nerve cell perikarya in the myenteric plexus of the P2X2 receptor-immunoreactive

neurons was not performed. The average nerve cell size of the NOS-immunoreactive neurons decreased in the sham 1 week group by 13% compared to the sham 24 h group and increased by 25% in the I/R 1 week group compared to the sham and control groups ($P<0.05$; Table 4). The average size of the ChAT-immunoreactive neurons was not significantly different between the control and sham groups. The average size of the ChAT-immunoreactive neurons increased by 16% in the I/R 1 week group compared to size in the sham 1 week and I/R 24 hour groups ($P<0.05$; Table 4). We observed that the profile area of calretinin-immunoreactive neurons increased by 32% in the sham 1 week group compared to the area in the control group ($P<0.05$, Table 4). The average size of calbindin-immunoreactive neurons increased in the sham 24 hour and sham 1 week groups by 15% and 18%, respectively, compared to the size in the control group. The average size of calbindin-immunoreactive neurons increased in the I/R 1 week group by 23% compared to that in the I/R 24 h group ($P<0.05$; Table 4). The neuron size distributions in the myenteric plexus of the control, sham, and I/R groups are shown as histograms in Fig. 4.

Discussion

Chemical coding

Paulino et al. (2011) analyzed the effects of ischemia in the superior mesentery artery following 4 hours of reperfusion; however, the P2X2 receptor in the chemical coding of enteric neurons and enteric glial cells in the ischemia of the superior mesentery artery after prolonged reperfusion has not been analyzed. This present study demonstrated a decrease in enteric neuronal density, an increase in the size of the neuron, and a decrease in P2X2 receptor expression in myenteric neurons following 24 hours and 1 week of reperfusion after ischemia. In addition, we observed increased glial cell density following I/R. Ventura-Martinez et al. (2008) showed the effects of ischemia for 5, 10, 20, 40, 80, or 160 min in the myenteric plexus. They found structural changes that started after 10 min of ischemia, which included cell swelling, vacuolization, and disruption of the protoplasmic and mitochondrial membranes.

We used NOS immunoreactivity to identify inhibitory motor neurons, ChAT and calretinin immunoreactivity to identify excitatory neurons, and calbindin immunoreactivity to identify intrinsic afferent neurons. The use of these identification markers in the rat ileum is consistent with other studies in rats and small mammals (Mann et al., 1999; Furness, 2006). The morphological analyses demonstrated that NOS-immunoreactive neurons exhibited Dogiel type I morphologies, whereas calretinin-immunoreactive neurons presented Dogiel type II morphologies. Calbindin-immunoreactive neurons exhibited Dogiel type I (small and elongated) and Dogiel type II (large and smooth) morphologies. These findings are consistent with previously published findings (Sayeg and Ritter, 2003). Talapka et al. (2011) demonstrated the presence of subcellular NOS isoforms in the duodenum of rats. Using electron microscopy and antibodies against neuronal NOS (nNOS), endothelial NOS (eNOS) and inducible NOS (iNOS), they showed that nNOS, eNOS and iNOS were expressed in myenteric neurons, smooth muscle, and the endothelium of capillaries. NADPH-diaphorase staining can be used for as a marker NOS immune reactivity. The expression of NADPH-diaphorase was assessed in the jejunum of rats after ischemia and reperfusion. After one hour of ischemia and 1 hour of reperfusion, changes were observed in the form of myenteric neurons and the intensity of labeling; 24 hours after reperfusion, NADPH-diaphorase activity returned but was low when compared to the control group; while 30 days after reperfusion, the histochemical changes had returned to the levels of the control group (Bolekova et al., 2011).

In the gastrointestinal tract, S100β is considered to be exclusively localized to glial cells (Ferri et al., 1982; Rühl, 2005). The use of S100β as a pan-glial marker for quantitative analyses is recommended given that S100β provides distinct and easily distinguished profiles of the glial soma that can be resolved and counted. In our work, the staining of glial cells in the ileum is consistent with previously published results (Ferri et al., 1982; Rühl, 2005). In the I/R groups, the density of glial cells was increased compared to the control and sham groups.

ATP depolarizes 70-90% of guinea pig enteric neurons, indicating that the majority of myenteric neurons express the P2X2 receptor (Barajás-Lopes et al., 1999; Bian et al., 2000; Galligan, 2002). In our work, we confirmed the presence of the P2X2 receptor in myenteric neurons colocalized for NOS, ChAT, calretinin, and calbindin neurons. Previous studies have demonstrated the presence of P2X2, P2X3, P2X6, and P2X7 receptor expression in the enteric nervous system of guinea pigs (Vulchanova et al., 1996; Hu et al., 2001; Castelucci et al., 2002a; Poole et al., 2003; Van Nassauw et al., 2002; Xiang and Burnstock, 2005), rats (Xiang and Burnstock, 2004; Yu et al., 2010), and mice (Giaroni et al., 2002; Ruan and Burnstock, 2005). Here, we observed the presence of the P2X2 receptor in both the cytoplasm and membrane of the myenteric neurons of control and sham animals, whereas a decrease in the immunoreactivity of the P2X2 receptor was revealed in the intestinal I/R group. These findings are in agreement with the work of Paulino et al. (2011).

Previous studies have demonstrated that most NOS-, ChAT-, calretinin-, and calbindin-immunoreactive neurons express the P2X2 receptor (Castelucci et al., 2002a; Paulino et al., 2011; Mizuno et al., 2012; Girotti et al., 2013). Our results are consistent with previous work demonstrating the presence of P2X2 in inhibitory, intrinsic afferent, and excitatory neurons. The study of colocalization in the myenteric neurons demonstrated that I/R does not change the neuronal neurochemical

code; this finding is consistent with the results of Paulino et al. (2011).

Interestingly, 12% of cells that were immunoreactive for the P2X2 receptor were not HuC/D positive (pan-neuronal) and thus may be another type of cell. To further investigate this result, we applied the dual-labeling of the P2X2 receptor with S100β, which is pan-glial for enteric glial cells. Our results showed that the majority of S100β-immunoreactive enteric glial cells were immunoreactive for the P2X2 receptor in the control, sham 24 hour, I/R 24 hour, sham 1 week, and I/R 1 week groups. A previous immunohistochemical studies demonstrated the presence of the P2X7 receptor in enteric glial cells (Vanderwinden et al., 2003) and indicated a developmental role for P2X7 in glial cells (Gulbransen and Sharkey, 2012). Additional work demonstrated that enteric glia cells were capable of detecting ATP released from neurons and were immunoreactive for the P2Y4 and P2Y11 receptors (Van Nassauw et al., 2006). Furthermore, studies using enteric glial cell cultures devoid of neurons together with a combination of Ca^{2+} imagining techniques showed that enteric glia from humans and rats were directly activated by neurotransmitters, such as ATP, 5-HT, and acetylcholine, involved in fast excitatory neurotransmission in the enteric nervous system (Gulbransen and Sharkey, 2009; Boesmans et al., 2013).

After abdominal surgery, intestinal hypomotility may occur in the manipulated area and can lead to stasis in the gut (Lubbers et al., 2010). In our work, the sham-operated groups were subjected to identical manipulations to the I/R groups without the arterial occlusion. In the control group, animals were not submitted to manipulation. We observed alterations in the neurons and glial cells of the sham-operated animals in the 24 hour and 1 week groups compared to controls; this suggests that both intestine manipulation and the I/R can affect the ileum (Thacker et al., 2011).

Interstitial cells of Cajal (ICC) are pacemakers of the gastrointestinal tract that form an extensive network between the circular and longitudinal layers at the myenteric plexus level (Mostafa et al, 2010). Shimojina et al. (2006) studied the effect of I /R on intestinal motility in the interstitial cells of Cajal (ICC) and showed that 80 minutes of ischemia with a reperfusion period of 12 hours produced a 25% reduction in the frequency of intestinal contractions associated with a 70% decrease in the markup of interstitial cells of Cajal. Four days after reperfusion, the pattern of motion and the ICCs recovered, suggesting that ICCs play an important role in the termination and recovery of gastrointestinal motility. Yano et al. (1997) investigated the relationship between the duration of ischemia and the effect on enteric ganglia, and they observed that an ischemic duration of 2 to 4 hours reduced the number neurons and could affect the intestinal peristalsis.

Changes in neuronal density

Changes in the density of the enteric nervous system have been observed in various regions of the gastrointestinal tract in rat models of undernourishment and refeeding (Castelucci et al., 2002b; Gomes et al., 2006; Misawa et al., 2010; Girotti et al., 2013). I/R protocols have also been shown to affect the density of enteric neurons (Calcina et al., 2005; Lindestron and Ekblad, 2004; Paulino et al., 2011; Palombit et al., 2013). In our work, the density of NOS-positive neurons decreased in the I/R 1 week group. Paulino et al. (2011) and Palombit et al. (2013) showed that NOS-immunoreactive neurons decreased following reperfusion. I/R causes neurons to lose their Ca^{2+} regulatory mechanisms, with one consequence being that Ca^{2+} moves down its concentration gradient from the extracellular fluid and enters the cell, increasing the cytoplasmic Ca^{2+} concentration (Dong et al., 2006). This increased cytoplasmic Ca^{2+} is predicted to activate NOS, a Ca^{2+}-dependent enzyme that appears to contribute to cell damage (Dong et al., 2006). As NOS is a Ca^{2+}-dependent enzyme, the loss of Ca^{2+} homeostasis following I/R may contribute to changes in the density of NOS-immunoreactive neurons.

The numbers of ChAT- and HuC/D-immunoreactive neurons (neurons/cm^2) was reduced following I/R for 24 hours and 1 week. The calretinin-immunoreactive neurons increased only in the I/R 1 week group. The calretinin- and calbindin-immunoreactive neurons appeared to be more resistant to the loss of Ca^{2+} homeostasis. It has been suggested that Ca^{2+}-binding proteins have a protective role in neurons (Baimbridge et al., 1995; D'Orlando et al., 2001).

Protocols involving low-protein dietary regimens may affect the expression of the P2X2 and P2X7 receptors in the enteric neurons of small (Misawa et al., 2010) and large intestines (Girotti et al., 2013). Models of female ob/ob mice have increased numbers of P2X2-immunoreactive ileum myenteric neurons (Mizuno et al., 2012). We found that neurons expressing the P2X2 receptor were decreased in the I/R groups. Previous studies demonstrated a decrease in the density of P2X2- and P2X7-immunoreactive neurons following I/R (Paulino et al., 2011; Palombit et al., 2013). In cases of injuries, such as intestinal ischemia, a large extracellular release of ATP, adenosine, and other neurotransmitters may occur, which are related to changes in receptor expression; further, P2 complex-specific responses in different cell types may occur, which may be related to adverse and/or beneficial effects (Franke et al., 2006). It is possible that depending on the protocol, circulating ATP levels may increase over a short or long time frame, which may result in changes in P2X receptor expression in neurons of the gastrointestinal tract and may ultimately reflect the purinergic signaling demand (Burnstock, 2014).

Apoptosis is an important process in chronic and acute ischemia. The modulation of P2 receptors is involved in excitotoxic necrosis and degeneration by apoptosis, possibly as a common signal transduction mechanism (Franke et al., 2006). The MAPK family, including ERK and p38, has been implicated in the

regulation of apoptosis through processes involving the P2X2 receptor (Fujita et al. 2000). There is an important switch between factors that activate ERK and stress factors that activate the JNK pathway or p38 that is important in determining whether a cell will survive or die. Additionally, Kawamura et al. (2010) demonstrated a relationship between purinergic receptors and pannexin. The P2X7 receptor association with pannexin contributes to the process of cell death in several ischemia processes (Locovei et al., 2007; Pelegrin and Supernant, 2006; Silverman et al., 2009). Results from our group have demonstrated that neurons of the myenteric plexus of the ileum that were immunoreactive to Hu completely colocalize with the P2X7 receptor (Palombit et al., 2013). Because the ileal neurons express the P2X7 receptor, interaction with pannexin-1 could contribute to events leading to neuronal death.

The density of S100β-immunoreactive enteric glial cells was increased following I/R. Studies have shown that different protocols have varied effects on enteric glial cells. Previous studies of I/R found distorted glia cells with 3 hours of ischemia until 12 hours of reperfusion (Thacker et al., 2011). Other authors demonstrated a loss of glial cells in the small and large intestines of aged rats (Phillips et al., 2004). Dietary restriction led to dramatically decreased glial populations (Cirilo et al., 2013). In the inflamed intestines of Crohn's disease, a high increase of GFAP in enteric glial cells compared to controls has been reported (Boyen et al., 2011). Stenkamp-Strahm et al. (2013) showed that a high-fat diet caused a significant decline in the area density indices of mucosa-associated glial cell networks in mice, as evidenced by S100Bβ staining at 8 and 20 weeks.

Changes in the neuronal size of myenteric neurons following I/R

Previous reports using various protocols, such as malnutrition (Castelucci et al., 2002b; Gomes et al., 2006; Misawa et al., 2010; Girotti et al., 2013), obesity (Mizuno et al., 2012), and I/R (Paulino et al., 2011; Palombit et al., 2013), have demonstrated effects on the neuronal size of the enteric neurons. We found that the neuronal profile area of neurons expressing NOS was increased in animals exposed to I/R in the 1 week group. These findings are in agreement with the results of Rivera et al. (2009) and Palombit et al. (2013) but not those of Paulino et al. (2011), who reported a decreased neuronal size. These discrepancies may be explained by the different periods of reperfusion that were analyzed. Furthermore, I/R causes Ca^{2+} to move down its concentration gradient from the extracellular fluid to enter the cell; the increased cytoplasmic Ca^{2+} inside the cell activates NOS, a Ca^{2+} dependent enzyme, producing NO, which can react with reactive oxygen species to produce peroxynitrite. This effect is consistent with the increased NOS-immunoreactive neuron profile area (Dong et al., 2006; Rivera et al., 2012).

Acetylcholine is one of the major transmitters in enteric neurons and is found in the excitatory motor neurons and intrinsic afferent neurons (Mann et al., 1999; Qu et al., 2008). ChAT-immunoreactive neurons were increased in animals exposed to I/R in the 1 week group. These findings are in agreement with previously published results (Palombit et al., 2013). Calbindin-immunoreactive neurons increased in size following I/R. In the ileum, approximately 80% of Dogiel type II neurons are immunoreactive for calbindin (Mann et al., 1999). Calretinin-immunoreactive neurons did not show a change in the profile area in the I/R groups compared to the sham groups. Calretinin is another Ca^{2+}-binding protein that plays a role in the transport and buffering of Ca^{2+}, perhaps via the ability to buffer the cytosolic Ca^{2+} increase in response to the inflow of Ca^{2+} following I/R; this finding is in agreement with the results of Rivera et al. (2009).

The present study demonstrates that ischemia followed by long periods of reperfusion may differentially affect the density and profile of enteric neurons and glial cells expressing the P2X2 receptor. These findings have clinical relevance to potential therapies for intestinal pathologies.

Acknowledgements. We thank Professors Jackson Cioni Bittencourt and Carol Fuzeti Elias for the use of a fluorescence microscope for certain analyses and Rosana Prisco for performing the statistical analysis. These studies were supported by the São Paulo Research Foundation (FAPESP/Fundação de Amparo à Pesquisa do Estado de São Paulo), the CNPq (Conselho Nacional de Desenvolvimento Científico e Tecnológico) and CAPES.

Conflict of interest. The authors have no conflict of interest.

References

Abbracchio M.P., Burnstock G., Verkhratsky A. and Zimmermann H. (2009). Purinergic signaling in the nervous system: an overview. Trends Neurosci. 32, 19-29.

Barajas-López C., Huizinga J.D., Gerzanich V., Espinosa-Luna R. and Peres A.L. (1996). P2X-purinoceptors of myenteric neurones from the guinea-pig ileum and their unusual pharmacological properties. Br. J. Pharmacol. 119, 1541-1548.

Baimbridge K.G., Celio M.R. and Rogers J.H. (1992). Calcium-binding proteins in the nervous system. Trends Neurosci. 15, 303-308.

Bian X.C., Bertrand P.P. and Bornstein J.C. (2000). Descending inhibitory reflexes involve P2X receptor–mediated transmission from interneurons to motor neurons in guinea-pig ileum. J. Physiol. 528, 551-560.

Boesmans W., Cirillo C., Van den Abbeel V., Van den Haute C., Depoortere I., Tack J. and Vanden Berghe P. (2013). Neurotransmitters involved in fast excitatory neurotransmission directly activate enteric glial cells. Neurogastroenterol. Motil. 25, 151-160.

Bolekova A., Spakovska T., Kluchova D., Toth S. and Vesela J. (2011). NADPH-diaphorase expression in the rat jejunum after intestinal ischemia/reperfusion. Eur. J. Histochem. 55, e23.

Boyen G.T. Von, Schulte N., Pflüger C., Spaniol U. and Hartmann

Steinkamp M. (2011). Distribution of enteric glia and GDNF during gut inflammation. BMC Gastroenterology 11, 3-8.

Burnstock G. (2014) Purinergic signaling in the gastrointestinal tract and related organs in health and disease. Purinergic Signal. 10, 3-50.

Calcina F., Barocelli E., Bertoni S., Furokawa O., Kaunitz J., Impicciatore M. and Sternini C. (2005). Effect of n-methyl-d-aspartate receptor blockade on neuronal plasticity and gastrointestinal transit delay induced by ischemia/reperfusion in rats. Neuroscience 134, 39-49.

Castelucci P., Robbins H.L., Poole D.P. and Furness J.B. (2002a). The distribution of purine P2X2 receptors in the guinea pig enteric nervous system. Histochem. Cell Biol. 117, 415-422.

Castelucci P., De Souza R.R., De Angelis R.C., Furness J.B. and Liberti E.A. (2002b). Effects of pre- and postnatal protein deprivation and postnatal re-feeding on myenteric neurons of the rat large intestine: a quantitative morphological study. Cell Tissue Res. 310, 1-7.

Cirilo C.P., Schoffen J.P., de Santi-Rampazzo A.P., Zapater M.C., Vicentini F.A., Comar J.F. and Natali M.R. (2013). Dietary restriction interferes with oxidative status and intrinsic intestinal innervation in aging rats. Nutrition 29, 673-680.

D'Orlando C., Fellay B., Schwaller B., Salicio V., Bloc A., Gotzos V. and Celio M.R. (2001). Caretinin and Calbindin D-28k delay the onset of cell death after excitotoxic stimulation in transfected P19 cell. Brain Res. 909, 145-158.

Dong Z., Saikumar P., Weinberg J.M. and Venkatachalam MA. (2006). Calcium in cell injury and death. Annu. Rev. Pathol. Mech. Dis. 1, 405-434.

Franke H., Krügel U. and Illes P. (2006). P2 receptors and neuronal injury. Pflugers Arch, 452, 622-644.

Ferri G.L., Probert L., Cocchia D., Michetti F., Marangos P.J. and Polak J.M. (1982). Evidence for the presence of S-100 protein in the glial component of the human enteric nervous system. Nature 297, 409-410.

Fujita N., Kakimi M., Ikeda Y., Hiramoto T. and Suzuki K. (2000). Extracellular ATP inhibits starvation-induced apoptosis via P2X2 receptors in differentiated rat pheochromocytoma PC12 cells. Life Sci. 31, 66(19), 1849-1859.

Furness J.B. (2006). The enteric nervous system. Blackwell publishing.

Gabella G. (1972). Fine structure of the myenteric neurons in the guinea-pig ileum. J. Anat. 111, 69-97.

Galligan J.J. (2002). Ligand-gated ion channels in the enteric neurvous sytem. Neurogastroenterol. Motility 14, 611-623.

Giaroni C., Knight G.E., Ruan H.Z., Glass R., Bardini M., Lecchini S., Frigo G. and Burnstock G. (2002). P2 receptors in the murine gastrointestinal tract. Neuropharmacology 43, 1313-1323.

Girotti P.A., Misawa R., Palombit K., Mendes C.E., Bittencourt J.C. and Castelucci P. (2013). Differential effects of undernourishment on the differentiation and maturation of rat enteric neurons. Cell Tissue Res. 353, 367-380.

Gomes O.A., Castelucci P., Fontes R.B.V. and Liberti E.A. (2006). Effects of pre- and postnatal protein and postnatal re-feeding on myenteric neurons of the rat small intestine: a quantitative morphological study. Auton. Neurosci. 126, 277-284.

Gulbransen B.D. and Sharkey K.A. (2009). Purinergic neuron-to-glia signaling in the enteric nervous system. Gastroenterology. 136, 1349-1358.

Gulbransen B.D. and Sharkey K.A. (2012). Novel functional roles for enteric glia in the gastrointestinal tract. Nat. Rev. Gastroenterol Hepatol. 9, 625-632.

Hu H.Z., Gao N., Lin Z., Liu S., Ren J., Xia Y. and Wood J.D. (2001). P2X7 receptors in the enteric nervous system of guinea-pig small intestine. J. Comp. Neurol. 440, 299-310.

Kawamura M. Jr, Ruskin D.N. and Masino S.A. (2010). Metabolic autocrine regulation of neurons involves cooperation among pannexin hemichannels, adenosine receptors, and KATP channels. J Neurosci. 30, 3886-3895

Lindestrom L. and Ekblad E. (2004). Structural and neuronal changes in rat ileum after ischemia with reperfusion. Dig. Dis. Sci. 49, 1212-222.

Locovei S., Scemes E., Qiu F., Spray D.C. and Dahl G (2007). Pannexin1 is part of the pore forming unit of the P2X(7) receptor death complex. FEBS. Lett. 581, 483-8.

Lubbers T., Burnman W. and Luyer M. (2010). Controlling postoperative ileus by vagal activation. World J. Gastroenterol. 16, 1683-1687.

Mann P.T., Furness J.B. and Southwell B.R. (1999). Choline acethyltransferase immunoreactivity of putative intrinsic primary afferent neurons in the rat ileum. Cell Tissue Res. 297, 241-248.

Misawa R., Girotti P.A., Mizuno M.S., Liberti E.A., Furness J.B. and Castelucci P. (2010). Effects of protein deprivation and re-feeding on P2X2 receptors in enteric neurons. World J. Gastroenterol. 16, 3651-3663.

Mizuno M.S., Crisma A.R., Borelli P. and Castelucci P. (2012). Expression of the $P2X_2$ receptor in different classes of ileum myenteric neurons in the female obese ob/ob mouse. World J. Gastroenterol. 18, 4693-703.

Mostafa R.M., Moustafa Y.M. and Hamdy H. (2010). Interstitial cells of Cajal, the Maestro in health and disease. World J. Gastroenterol. 16, 3239-3348.

Oldenburg W.A., Lau L.L., Rodenberg T.J., Edmonds H.J. and Burger C.D. (2004). Acute mesenteric ischemia: A clinical review. Arch. Intern. Med. 164, 1054-1062.

Palombit K., Mendes C.E., Tavares-de-Lima W., Silveira M.P. and Castelucci P. (2013). Effects of ischemia and reperfusion on subpopulations of rat enteric neurons expressing the P2X7 receptor. Dig. Dis. Sci. 58, 3429-39.

Paulino A.S., Palombit. K., Cavriani G., Tavares-de-Lima W., Mizuno M.S., Marosti A.R., da Silva M.V., Girotti P.A., Liberti E.A. and Castelucci P. (2011). Effects of ischemia and reperfusion on P2X2 receptor expressing neurons of the rat ileum enteric nervous system. Dig. Dis. Sci. 56, 2262-2277.

Pelegrin P. and Surprenant A. (2006). Pannexin-1 mediates large pore formation and interleukin-1beta release by the ATP-gated P2X7 receptor. EMBO J. 25, 5071-5082.

Phillips R.J., Kieffer E.J. and Powley T.L. (2004). Loss of glia and neurons in the myenteric plexus of the aged Fischer 344 rat. Anat. Embryol. (Berl). 209, 19-30.

Piao D.X., Jiang C.H., Kosata M., Shibata T., Ohtsuka A. and Murakami T. (1999). Cytoplasmic delayed neuronal death in the myenteric plexus of the rat small intestine after ischemia. Arch. Histol. Cytol. 62, 383-392.

Poole D.P., Castelucci P., Robbins H.L., Chiocchetti R. and Furness J.B. (2002). The distribution of P2X3 purine receptor subunits in the guinea-pig enteric nervous system. Auton. Neurosci. 101, 39-47.

Qu Z.D., Thacker M., Castelucci P., Bagyánszki M., Epstein M.L. and Furness J.B. (2008). Immunohistochemical analysis of neuron types in the mouse small intestine. Cell Tissue Res. 334, 147-161.

Rivera L.R., Thacker M., Castelucci P., Bron R. and Furness J.B.

(2009). The reactions of specific neuron types to intestinal ischemia in the guinea pig enteric nervous system. Acta Neuropathol. 118, 261-270.

Rivera L.R., Pontell L., Cho H.J., Castelucci P., Thacker M., Poole D.P., Frugier T. and Furness J.B. (2012). Knock out of neuronal nitric oxide synthase exacerbates intestinal ischemia/reperfusion injury in mice. Cell Tissue Res. 349, 565-576.

Ruan H.Z. and Burnstock G. (2005). The distribution of P2X5 purinergic receptors in the enteric nervous system of mouse. Cell Tissue Res. 319, 191-200.

Rühl A. (2005). Glial cells in the gut. Neurogastroenterol. Motil. 17, 777-790.

Sayegh A.I. and Ritter R.C. (2003). Morphology and distribution of nitric oxide sinthase, neurokin-1 receptor, Calretinin, Calbindin, and neurofilament-M- immunoreactive neurons in the myenteric and submucosal plexuses of the rat small intestine. Anat. Rec. 271, 209-216.

Shimojima N., Nakaki T., Morikawa Y., Hoshino K., Ozaki H., Hori M. and Kitajima M. (2006). Interstitial cells of Cajal in dysmotility in intestinal ischemia and reperfusion injury in rats. J. Surg. Res. 135, 255-261.

Silverman W.R., de Rivero Vaccari J.P., Locovei S., Qiu F., Carlsson S.K., Scemes E., Keane R.W. and Dahl G. (2009) The pannexin 1 channel activates the inflammasome in neurons and astrocytes. J. Biol. Chem. 284, 18143-18151.

Stenkamp-Strahm C., Patterson S., Boren J., Gericke M. and Balemba O. (2013). High-fat diet and age-dependent effects on enteric glial cell populations of mouse small intestine. Auton. Neurosci. 177, 199-210.

Talapka P., Bódi N., Battonyai I., Fekete E. and Bagyánszki M. (2011). Subcellular distribution of nitric oxide synthase isoforms in the rat duodenum. World. J. Gastroenterol. 17, 1026-9.

Thacker M., Rivera L.R., Cho H.J. and Furness J.B. (2011). The relationship between glial distortion and neuronal changes following instestinal ischemia and reperfusion. Neurogastroenterol. Motil. 1, 1-10.

Vanderwinden J.M., Timmermans J.P. and Schiffmann S.N. (2003). Glial cells, but not interstitial cells, express P2X7, an ionotropic purinergic receptor, in rat gastrointestinal musculature. Cell Tissue Res. 312, 149-154.

Van Nassauw L., Brouns I., Adraensen D., Burnstock G. and Timmermans J.P. (2002). Neurochemical identification of enteric neurons expressing P2X(3) receptors in the guinea-pig ileum. Histochem. Cell Biol. 118, 193-203.

Van Nassauw L., Costagliola A., Van Op den Bosch J., Cecio A., Vanderwinden J.M., Burnstock G. and Timmermans J.P. (2006). Region-specific distribution of the P2Y4 receptor in enteric glial cells and interstitial cells of Cajal within the guinea-pig gastrointestinal tract. Auton. Neurosci. 126, 299-306.

Van L., Costagliola A., Van Op den Bosch J., Cecio A., Vanderwinden J.M., Burnstock G. and Timmermans J.P. (2006). Region-specific distribution of the P2Y4 receptor in enteric glial cells and interstitial cells of Cajal within the guinea-pig gastrointestinal tract. Auton. Neurosci. 126, 299-306.

Ventura-Martinez R., Santiago-Mejia J., Gomez C., Rodriguez R. and Fortoul T.I. (2008). Acute morphological changes in guinea-pig ileum myenteric neurons after ischemia in situ with superfusion in vitro. Pathol. Res. Pract. 204, 121-7.

Vulchanova L., Arvidsson U., Riedl M., Wang J., Buell G., Suprenant A. and Nort R.A. (1996). Differential distribution of two ATP-gated ion channels (P2x receptors) determined by immunohistochemistry. Proc. Natl. Acad. Sci. USA 93, 8063-8067.

Xiang Z. and Burnstock G. (2004). P2X2 and P2X3 purinoceptors in the rat enteric nervous system. Histochem. Cell Biol. 12, 169-179.

Xiang Z. and Burnstock G. (2005). Distribution of P2Y2 receptors in the guinea pig enteric nervous system and its coexistence with P2X2 and P2X3 receptors, neuropeptide Y, nitric oxide synthase and calretinin. Histochem. Cell Biol. 124, 379-390.

Yano K., Hosokawa K. and Hata Y. (1997). Quantitative morphology of Auerbach's plexus in rat intestinal wall undergoing ischemia. J. Reconstr. Microsurg. 13, 297-301.

Yu Q., Zhao Z., Sun J., Guo W., Fu J., Burnstock G., He C. and Xiang Z. (2010). Expression of P2X6 receptors in the enteric nervous system of the rat gastrointestinal tract. Histochem. Cell Biol. 133, 177-188.

Accepted November 17, 2014